Journal of Environmental Management 386 (2025) 125639

Contents lists available at ScienceDirect

Journal of Environmental Management

journal homepage: www.elsevier.com/locate/jenvman

Research article

Improving paper-based packaging with home compostable modified starch coatings: a focus on heat seal optimization

Azadeh Sadeghi [a,*], Farshad Abavisani [b], Amir Saffar [c], Abdellah Ajji [a,**]

[a] Département de Génie Chimique, Polytechnique Montréal, Montréal, QC, (H3C3A7), Canada
[b] Department of Bioresource Engineering, McGill University, Sainte-Anne-de-Bellevue, QC, (H9X3V9), Canada
[c] ProAmpac Inc., Boulevard des Entreprises, Terrebonne, QC, (J6Y 1V2), Canada

ARTICLE INFO

Handling editor: Lixiao Zhang

Keywords:
Sodium starch octenyl succinate (SSOS)
Maltodextrin (MAL)
Heat sealable
Optimization
Paper-based flexible packaging

ABSTRACT

In the quest for sustainable packaging solutions, this study pioneers the development of home-compostable coatings that transform the heat sealability of paper-based flexible food packaging—a longstanding challenge in the industry. Leveraging sodium starch octenyl succinate (SSOS) and maltodextrin (MAL), compostable starch derivatives, combined with sorbitol (SOR) and glycerol (GLY) as plasticizers, we optimized critical sealing parameters: seal initiation temperature (SIT) and fiber tear temperature (FTT). Using an innovative central composite design (CCD) and response surface methodology (RSM), the research reveals the interplay between material composition and sealing performance, uncovering unprecedented efficiency in achieving low SIT and FTT values. Remarkably, the optimal formulations achieved SIT and FTT values as low as 120 °C and 147 °C for SSOS (10 % SOR, 20 % GLY) and 112 °C and 125 °C for MAL (20 % SOR, 5 % GLY), outperforming traditional alternatives while maintaining full compostability. The statistical framework demonstrated exceptional predictive accuracy ($R^2 > 0.85$) and precision (CV < 7.4 %), underscoring the reliability and scalability of these formulations. This groundbreaking approach bridges the gap between sustainability and functionality, setting a new standard for home compostable packaging materials. By providing a scalable pathway to reduce environmental impact without compromising performance, this study offers transformative insights for the packaging industry and positions itself as a cornerstone for future innovations in sustainable food packaging.

1. Introduction

With the ongoing increase in the global population, there is a corresponding rise in the demand for food products and their packaging. A crucial challenge in food packaging is ensuring the preservation of quality, enhancing safety, and extending the shelf life of food items (Jahdkaran et al., 2021). Packaging must shield its contents from environmental influences like microorganisms, light, and external gases to prevent microbial and biochemical degradation. Thus, packaging should remain sealed until it is opened by the consumer for use (Bamps et al., 2023). Indeed, the product's shelf life is contingent upon the sealing quality of the flexible material (Merabtene et al., 2022). Flexible packaging is typically favored over rigid packaging due to its lighter weight and lower cost (Dudbridge, 2016). Lightweight materials like paper, plastic, and composites are suitable for flexible food packaging (Piergiovanni et al., 2016). Due to their lightweight nature, less energy is required for transportation. Flexible packaging holds approximately 30 % of the global market share, with food packaging being its primary application (Bamps et al., 2023).

In the food industry, plastic is predominantly employed for packaging purposes due to its cost-effectiveness, ease of processing, and widespread availability (Ganjizadeh et al., 2021). In general, petroleum-based synthetic polymers are extensively utilized in various packaging applications. However, their non-biodegradable nature leads to environmental challenges and heightens reliance on petroleum resources (Salwa et al., 2019).

Paper and cardboard are currently considered as the most widely used biodegradable materials for food packaging. Structurally, paper is simpler than plastic, suggesting migration of substances from the packaging into the food is likely to be lower compared to similar plastic

* Corresponding author.
** Corresponding author.
E-mail addresses: azadeh.sadeghi@polymtl.ca (A. Sadeghi), farshad.abavisani@mail.mcgill.ca (F. Abavisani), amir.saffar@proampac.com (A. Saffar), abdellah.ajji@polymtl.ca (A. Ajji).

https://doi.org/10.1016/j.jenvman.2025.125639
Received 29 December 2024; Received in revised form 22 March 2025; Accepted 30 April 2025
Available online 15 May 2025
0301-4797/© 2025 The Authors. Published by Elsevier Ltd. This is an open access article under the CC BY license (http://creativecommons.org/licenses/by/4.0/).

counterparts (Ganjizadeh et al., 2021). Nevertheless, paper and paper-based flexible packaging exhibits inadequate heat sealability (Deshwal et al., 2019). The low thermal conductivity of paper complicates effective sealing, requiring either prolonged sealing times or increased sealing temperatures (Hauptmann et al., 2021). These limitations present significant challenges for its utilization in packaging applications. Therefore, applying a coating (such as aluminum foil, plastic, and polymers) is the most straightforward method to enhance the functional properties of paper. However, these coatings can leach into food products, posing potential health risks, and interfere with the recycling process, thereby contributing to landfill waste increase (Deshwal et al., 2019; Thurber et al., 2020).

In order to select an appropriate coating for paper-based packaging, it is essential to consider both environmental concerns and heat-sealing properties of the coating. Heat sealing acts as a safeguard against microbial penetration through films and enhances both the barrier characteristics and mechanical strength of the films. In the heat sealing process, the polymer is heated to high temperatures until it melts and is then compressed under pressure (Lim et al., 2020). The heat sealing characteristics of polymers are influenced by surface chemistry of the materials (Allen, 1987). Moreover, the interaction between functional groups, such as -OH, -CHO, and -COOH, on a film affects seal strength (Rompothi et al., 2017). Seal strength is evaluated based on sealing temperature, pressure, and dwell time, all of which are crucial factors influencing its effectiveness. Among them, temperature is a very important parameter as using an incorrect sealing temperature can lead to a reduction in seal strength (Das et al., 2016). Therefore, it is essential to properly adjust the temperature.

Starch, a very popular compound, recognized for its status as a highly renewable and biodegradable natural polymer, is of particular academic interest due to its abundant availability, economic viability, non-toxic properties, and water solubility, rendering it a compelling candidate for diverse applications (Apriyanto et al., 2022; Zamani et al., 2023). Despite its potential, thermoplastic starch is less frequently employed due to challenges associated with solution viscosity, film formation, and retrogradation (Nechita et al., 2020). As a result, the use of modified starches is advocated to improve characteristics such as adhesion, solubility, and thermal resistance (He et al., 2023). Among the various modified starches, sodium starch octenyl succinate (SSOS) and maltodextrin (MAL) are particularly advantageous. They not only enhance the sealability of paper but also qualify as home-compostable materials.

SSOS, a derivative obtained through the esterification of native starch, has received approval from both the United States Food and Drug Administration (FDA) and the European Food Safety Authority (EFSA) for use in food products due to its non-toxic nature and biodegradability (Sajilata et al., 2005; Coggins, , 2000; Liu et al., 2013). This esterification process introduces the hydrophobic characteristics of the octenyl group while preserving the hydrophilic nature of the starch backbone, resulting in an amphiphilic molecule (Liu et al., 2013; Wang et al., 2011). MAL, synthesized through the acid or controlled enzymatic hydrolysis of starch, consists of D-glucose polymers linked by α-(1,4) and α-(1,6) bonds, and is characterized by its high water solubility and dispersibility (Du et al., 2021; Garnero et al., 2013). The degree of starch degradation in MAL is measured by the dextrose equivalent (DE) value, which assesses the concentration of reducing-end groups and is inversely related to the average degree of polymerization (DP) of the dehydrated glucose units (Xiao et al., 2022). With a DE value ranging from 3 to 20, MAL is characterized by long carbohydrate chains and a complex mix of high and low molecular weight substances (Parikh et al., 2014; Saavedra-Leos et al., 2015). Consequently, films made from this starch derivative can resemble multicomponent films in their properties (Liu et al., 2013).

Absence of plasticizers in starch films provokes a network with high cohesive energy caused by hydrogen bonds, resulting in a brittle structure (Suh et al., 2020). The incorporation of plasticizers disrupts intermolecular forces, increasing free volume and lowering the glass transition temperature (Tg), thus, enabling sealing at lower temperatures than conventional methods (Jiménez et al., 2013; Basiak et al., 2018; Alves et al., 2007). The efficacy of the film is profoundly affected by the specific type and concentration of plasticizer employed (Rompothi et al., 2017; Suh et al., 2020). In particular, the synergistic use of high molecular weight plasticizers, such as sorbitol (SOR), in conjunction with low molecular weight plasticizers, like glycerol (GLY), markedly enhances the functional properties of starch-based films (Muscat et al., 2012; MohammadiNafchi et al., 2010).

As stated, temperature is a critical parameter in heat sealing. The initiation temperature significantly affects seal strength, and a low seal initiation temperature (SIT) is regarded advantageous for a sealant layer (Morris, 2017; Herrera et al., 2016). However, if the seal temperature is too low, it can result in weak seals (Morris, 2022). Additionally, the layered network structure of paper makes it prone to fiber tearing, primarily due to mechanical interlocking. This occurs when the polymer sealant penetrates and intervenes in cellulose fibers, leading to their fracture and separation when seals are opened (Frihart, 2005). Achieving complete fiber tear is crucial for strong adhesive bonding in paper packaging (Kavčič et al., 2023), and monitoring fiber tear temperature (FTT) ensures quality by verifying seal strength and paper properties. Both SIT and FTT are essential for reliable heat sealing, impacting the performance and quality of final product in the packaging industry.

In this study, a central composite design (CCD) with rotatable and uniform precision, along with response surface methodology (RSM), was employed to examine how varying percentages of SOR and GLY affect the heat-sealing process (SIT and FTT) for each type of modified starch (SSOS and MAL) applied to paper. This investigation aims to examine the varying concentrations of plasticizers (SOR and GLY) in modified starches (SSOS and MAL) for enhancement in the sealability of paper-based packaging. Additionally, the rigorously designed experimental framework is anticipated to furnish predictive capabilities for analogous systems and contribute to a more comprehensive understanding of the multifactorial interactions that improves the heat sealability of paper-based packaging materials. In fact, this product is engineered to mitigate environmental impact and uphold food safety standards, thereby highlighting it among other commercially available compostable or biodegradable alternatives.

2. Experimental section

2.1. Materials

The sodium starch octenyl succinate (SSOS; E 1450) used in this study was purchased from Chanjao Longevity Co., Ltd. Bangkok, Thailand (Myskinrecipes Co.). Maltodextrin (MAL), with a dextrose equivalent (DE) of 10, was sourced from the Toronto Brewing Company, ON, Canada. Additionally, sorbitol (SOR) and glycerol (GLY) were obtained from Sigma-Aldrich, ON, Canada. Bleached paper with 5.5 % moisture, a tensile strength (MD) of 20 lbf/in, and tear strengths (CD and MD) of 30 gf and 24 gf, respectively, was supplied by Prolamina Corp (U. S.).

2.2. Preparation of biopolymer coatings on paper

The coatings were formulated using modified starches, specifically SSOS and MAL, along with SOR and GLY as plasticizers. The formulation process involved stirring the mixture for 1.5 h at room temperature, using distilled water as the solvent. The total biopolymer concentration was set at 25 % (w/w) in the casting solution. The plasticizer content was varied from 0 to 20 % (w/w) of the polymer concentration, as outlined in Tables 1 and 2 (a and b), according to the design of experiments (DOE) results generated with JMP statistical software (Version pro-17). The DOE assessed the effects of SOR, GLY, and their interactions to optimize the outcomes of the coating formulation.

Table 1
The input variables and their levels CCD employed.

Independent Variables	Type	Coded levels				
		−1.4	−1	0	+1	+1.41
X_1: Sorbitol (wt %)	Continuous	0	2.93	10	17.07	20
X_2: Glycerol (wt %)	Continuous	0	2.93	10	17.07	20

After preparing the casting solution, it was left to stand for 1 h to eliminate bubbles and ensure uniformity. The film solution was then applied to paper substrates using a bar coater machine (TQC Sheen AB4120) with a Mayer rod, producing a 2 μm wet film thickness, and the substrates were simultaneously dried for 2 min using an infrared (IR) dryer (Datous Boss, ZJ-SC-002, 2 kW, 220V) to set the coating. The process was then repeated under identical conditions, applying a second layer with the Mayer rod to achieve a 4 μm wet film thickness, followed by simultaneous drying.

2.3. Evaluation of heat sealing

Heat sealing evaluations were carried out utilizing an SL10 LakoTool laboratory hot-tack and seal tester, sourced from Lako Tool & Manufacturing Inc. The tests were executed at a pressure of 40 psi with a dwell time of 1.5 s (1500 ms) across various temperatures. Following the sealing process, peel tests were conducted at a speed of 33 mm/s to evaluate the seal quality. Each sample, measuring 7 inches by 1 inch, was tested using an Instron machine (model E3000). The peel test for each sample was conducted 10 times, with results for the seal initiation temperature (SIT) and fiber tear temperature (FTT) documented.

2.4. Physical properties

The coating weight of the coating layer was determined by measuring the mass of paper samples before and after the coating process (Quintix 224-1S, Sartorius Mechatronics).

2.5. Experimental design

2.5.1. Selection criteria of parameters

Numerous factors can influence seal strength and integrity during heat sealing, including material properties (such as branching, sealant thickness, and molecular weight) and process parameters (such as temperature, dwell time, and pressure) (Ilhan et al., 2021).The current project's primary goal is to develop a home compostable heat-sealable coating for paper-based flexible packaging. To minimize overall energy consumption and reduce greenhouse gas emissions, it is crucial to reduce the coating weight. Implementing an experimental design that includes all these parameters is challenging due to time, material costs, and data analysis complexities. Therefore, based on findings from the literature, we reduced the number of factors. Preliminary experiments were conducted to find an optimal condition for achieving a lower coating weight (3–3.80 $\frac{g}{m^2}$), as shown in Table 2 a and b for each modified starch, with bar coating speeds of 150 mm/s, specific wire sizes of 2 and 4 μm (wet film thickness), and a total polymer concentration of 25 % (w/w).

Pretests on the impact of plasticizer content revealed that increasing its percentage beyond 20 % did not significantly affect sealing quality. Consequently, higher amounts of plasticizer were excluded from the experimental design. Our study focuses on examining plasticizer percentages within the range of 0–20 % (w/w).

2.5.2. Optimization by central composite design (CCD)

The Response Surface Methodology (RSM) was conducted using a rotatable and uniform precision central composite design (CCD) to identify the optimal conditions for minimizing both the SIT and the FTT. In fact, RSM encompasses a collection of mathematical and statistical techniques designed to model and analyze the relationships between a set of input and response variables (Jadaa et al., 2020). By applying RSM, a polynomial equation can be fitted to the experimental data, allowing for the evaluation of interaction and quadratic effects among the tested factors. Additionally, RSM offers the advantage of reducing the number of experiments needed by eliminating those that are unnecessary (Sudarjanto et al., 2006; Bagheri et al., 2016). Moreover, the rotatability of the design ensure consistent prediction variance at all levels, as they are equidistant from the central point (Myers, , 2016). In addition, the uniform precision of the design provided for consistent prediction accuracy across the entire experimental space, enhances the reliability of the model. In this research, following the optimization of the coating weight, the influence of the percentage of SOR (X_1,%) and the percentage of GYL (X_2,%), as continuous independent input variables, on the minimum SIT (Y_1, °C) and the minimum FTT (Y_2, °C) was investigated via JMP software. It is noteworthy that the randomization of the experiments was carried out to ensure the minimization of unknown variability for the actual response which could caused by uncharted factors. The coded variables (X_i) for the CCD were determined using Equation (1) (Jadaa et al., 2020):

$$X_i = \left(\frac{x_i - x_0}{\Delta x}\right) \tag{1}$$

Where X_i denotes the dimensionless coded value of a variable; x_i represents the actual value of the variable; x_0 is the value of x at the center point; and Δx signifies the step change.

The coded levels of the two independent variables are detailed in Table 1. In this table, the values (+1) and (−1) correspond to the high and low levels of the two-level factorial design, respectively. (+1.41) and (−1.41) values represent the levels of axial point, while the value (0) indicates the center point of the experimental design.

The CCD comprises a total of 10 experiments for each modified starch (SSOS and MAL), organized as follows: (i) four points by a two-level full factorial design experiment, (ii) four axial points, and (iii) two central points. To assess the pure error of the experiments, the latter experiments corresponding to the center point were replicated two times led to 20 tests in total.

The data obtained from the CCD were analyzed using a second-degree polynomial regression analysis to elucidate the system's behavior. This function was chosen to gain a proper fitness maintaining a high significance with a simple function possible. This analysis was conducted using the least squares regression methodology, as depicted in Equation (4.2) (Moussa et al., 2022).

$$y_i = \beta_0 + \sum_{j=1}^{K} \beta_j x_{i,j} + \sum_{j=1}^{K-1} \sum_{K=j+1}^{K} \beta_{ijK} x_{i,j} x_{i,k} + \sum_{j=1}^{K} \beta_{jj} x_{i,j}^2 \tag{2}$$

In which y_i is the response of SIT and FIT, K represents the number of continuous variables; β_0 , β_j, β_{ijK} and β_{jj} are the estimated constant, linear, interaction, and quadratic coefficients effects, respectively. The factors are represented by actual variables, such as $x_{i,j}, x_{i,k}, x_{i,j}^2$.

2.5.3. Statistical optimization and validation

To identify the optimal levels of the two independent variables (x_1 and x_2) for achieving the desired response goals, both individual and comprehensive optimization procedures were performed. Additionally, the adequacy of the regression equations was assessed by comparing the experimental data to the predicted values from these equations. The results were analyzed using analysis of variance (ANOVA), and surface responses were displayed. Moreover, the least squares regression method was employed to develop multivariate models for the responses. These reduced response models were visually represented as 3D surface plots, illustrating how the interaction between the independent variables affected SIT and FTT parameters.

To verify the optimized data two different approaches were implemented. First, a 95 % prediction interval (PI) for each response was calculated by JMP using Equation (3) (Montgomery, 2017).

$$PI = \widehat{Y} \pm t \times s\sqrt{\left(1 + x_0'(\boldsymbol{X}'\boldsymbol{X})^{-1}x_0\right)} \quad (3)$$

In this formula, t represents the t-value of the predicted response from the t-distribution, s is the standard deviation of the predicted response, x_0 is vectors containing the model terms for each run, x_0' is its transpose form, $\boldsymbol{X}$ is the design matrix, and $\boldsymbol{X}'$ is also its transpose matrix. To validate the model, a single confirmation run was conducted for each set of optimal data using the input values recommended by the model, ensuring that they fell within the specified PI range.

In the second approach, more confirmation runs were carried out to check the occurrence of any alterations between the initial experiment and follow-up runs that could lead to a shift in the response defined as block effect (Mee, 2009). Furthermore, statistical confidence interval (CI) at a 99 % confidence level for the mean response was calculated through a method suggested by Antony using Equation (4) (Antony, 2023).

$$CI = \bar{y} \pm 3\left\{\frac{SD}{\sqrt{n}}\right\} \quad (4)$$

Where $\bar{y}$ represents the mean response obtained from confirmation trials or runs, SD is the standard deviation of the response derived from these trials, and n denotes the number of samples (or confirmation runs) conducted. This step is essential for providing the necessary parameters to assess the variability and reliability of the mean response in the context of the experimental data.

3. Results and discussion

3.1. Statistical analysis

3.1.1. Experimental design fitting

Table 2 (a and b) presents the actual values of for SSOS and MAL level, respectively, as well as all experimental (20 runs) with related observed and predicted data for SIT (Y_1), FTT (Y_2), and corresponding desirability scores based on the predicted data. It is important to highlight that the least squares regression method was utilized to develop multivariate models for the responses.

The results show the predicted values are generally close to the observed values, suggesting good accuracy of the predictive model. For instance, in SSOS (Table 2a) for run 1, 5, 9, 14, 15, 17, 18 and 20, the difference between predicted and observed values were below 5 °C for both SIT and FTT. This alignment in the results was also reflected in MAL data (Table 2b) where runs number 6, 7, 8, 9, 18, 17, and 18 represented the less than 5 °C difference between the values. In both modified starches, there was no run with more than 10 °C variation between the model outcomes and actual data. This strong match indicates that the model not only fits the data well but also has predictive validity.

The desirability score indicates the suitability of each experimental condition, with values closer to 1 representing more favorable outcomes. For SSOS results, scores range from 0.18 to 0.91, indicating varying levels of desirability for the conditions tested. Higher scores (e.g., 0.91 for Run 8 or run 15) suggest more optimal conditions with lower related SIT and FTT values, while lower scores (e.g., 0.18 for Runs 4 (or run 11)) indicate less favorable outcomes and higher SIT and FTT. Similarly, for MAL results, scores range from 0.22 to 0.98 where the highest score (0.98) occurred for Run 2 or Run 13, and the lowest scores (0.22) achieved in Runs 4 or Run 11 reflecting maximum and minimum desirability of outcomes, respectively.

The agreement between observed and predicted values was statistically evaluated using an Analysis of Variance (ANOVA), as detailed in Table 3. This statistical approach was applied to confirm the significance of the variables and their impact on the model. A second-order polynomial model was utilized to better understand the system, allowing for the examination of interaction effects among various variables. These interactions were analyzed by comparing the estimated coefficients, which provided insights into how the variables influence the studied responses.

The purpose of this analysis was to explore the relationship between the input factors and the key responses, specifically SIT (Y_1) and FTT (Y_2). By examining these relationships, the study aimed to determine the extent to which variations in the factors affect the responses. The results, outlined in Table 3 (a and b) for SSOS and MAL respectively, highlight how these factors interact and contribute to the overall properties of the coating formulation. This deeper understanding helps in optimizing the formulation to achieve the desired characteristics.

In Table 3 (a and b), x_1 and x_2 indicate the level of SOR and GYL, respectively, for each modified starch. Combined with the ANOVA results, the least significant variables were excluded from the model. In

Table 2a
CCD with two input variables (%SOR and %GLY), two output variables (SIT and FTT), desirability score, and coating weight for SSOS.

Run	Variables		Coating weight $\left(\frac{g}{m^2}\right)$	Response				Desirability score
	X_1 (%)	X_2 (%)		SIT (°C)		FTT (°C)		
				Observed	Predicted	Observed	Predicted	
1	0	10	3.52 ± 0.004	160	167	190	195	0.27
2	20	10	3.51 ± 0.003	160	153	175	168	0.57
3	2.93	17.07	3.28 ± 0.004	130	128	180	170	0.72
4	2.93	2.93	2.80 ± 0.008	190	187	210	202	0.18
5	10	10	3.23 ± 0.005	160	161	180	183	0.42
6	10	10	3.19 ± 0.001	170	161	185	183	0.42
7	17.07	17.07	3.66 ± 0.007	135	142	155	155	0.69
8	10	20	3.58 ± 0.006	125	120	140	146	0.91
9	10	0	3.21 ± 0.009	155	157	180	179	0.46
10	0	10	3.43 ± 0.006	160	167	190	195	0.27
11	2.93	2.93	2.59 ± 0.002	190	187	210	202	0.18
12	17.07	2.93	3.68 ± 0.008	140	144	160	166	0.63
13	20	10	3.23 ± 0.003	160	153	175	168	0.57
14	10	10	3.49 ± 0.02	165	161	180	183	0.42
15	10	20	3.28 ± 0.008	125	120	140	146	0.91
16	2.93	17.07	3.55 ± 0.005	130	128	180	170	0.72
17	17.07	17.07	3.58 ± 0.008	135	142	155	155	0.69
18	10	0	3.71 ± 0.008	155	157	180	179	0.46
19	17.07	2.93	3.28 ± 0.008	140	144	160	166	0.63
20	10	10	3.51 ± 0.005	160	161	180	183	0.42

Table 2b
CCD with two input variables (%SOR and %GLY), two output variables (SIT and FTT), desirability score and coating weight for MAL.

Run	Variables		Coating weight $\left(\frac{g}{m^2}\right)$	Response				Desirability score
	X_1 (%)	X_2 (%)		SIT (°C)		FTT (°C)		
				Observed	Predicted	Observed	Predicted	
1	0	10	3.45 ± 0.008	165	170	190	200	0.48
2	20	10	3.41 ± 0.007	125	118	135	129	0.98
3	2.93	17.07	3.38 ± 0.001	150	140	180	173	0.74
4	2.93	2.93	2.71 ± 0.006	230	224	255	245	0.22
5	10	10	3.28 ± 0.004	140	146	160	165	0.73
6	10	10	3.59 ± 0.001	140	146	160	165	0.73
7	17.07	17.07	3.56 ± 0.007	140	141	160	161	0.77
8	10	20	3.20 ± 0.003	140	142	170	173	0.71
9	10	0	3.01 ± 0.005	170	175	200	200	0.48
10	0	10	3.33 ± 0.005	165	170	190	200	0.48
11	2.93	2.93	2.81 ± 0.008	230	224	255	245	0.22
12	17.07	2.93	3.65 ± 0.005	135	128	150	145	0.88
13	20	10	3.43 ± 0.007	125	118	129	135	0.98
14	10	10	3.29 ± 0.01	140	146	160	165	0.73
15	10	20	3.40 ± 0.008	140	142	170	173	0.71
16	2.93	17.07	3.35 ± 0.001	150	140	180	173	0.74
17	17.07	17.07	3.38 ± 0.005	140	141	160	161	0.77
18	10	0	3.31 ± 0.006	170	175	200	200	0.48
19	17.07	2.93	3.85 ± 0.008	135	128	150	145	0.88
20	10	10	3.59 ± 0.001	140	146	160	165	0.73

Table 3a
ANOVA results for SIT and FTT by SSOS optimization. Significant effects ($p < 0.05$) are highlighted in bold.

AVOVA source (SSOS)	Sum of squares	D. F.	Mean square	F-ratio	*p*-value
SIT					
x_1: Sorbitol	506.25	1	506.25	9.349	0.0080
x_2: Glycerol	2885.108	1	2885.108	53.282	<0.0001
$x_1.x_2$	1512.5	1	1512.5	27.932	<0.0001
x_1^2	–	–	–	–	-
x_2^2	1508.928	1	1508.928	27.867	<0.0001
Lack of fit	712.213	4	178.053	19.585	
Pure error	100.00	11	9.091		
Total error	812.213	15			<0.0001
FTT					
x_1: Sorbitol	2314.245	1	2314.245	35.048	<0.0001
x_2: Glycerol	2096.199	1	2096.199	31.746	<0.0001
$x_1.x_2$	312.500	1	312.500	4.732	0.0460
x_1^2	–	–	–	–	–
x_2^2	1160.357	1	1160.357	17.573	0.0008
Lack of fit	971.698	4	242.925	142.515	
Pure error	18.750	11	1.705		
Total error	990.448	15		<0.0001	

Table 3b
ANOVA results for SIT and FTT by MAL optimization. Significant effects ($p < 0.05$) are highlighted in bold.

AVOVA source (MAL)	Sum of squares	D. F.	Mean square	F-ratio	*p*-value
SIT					
x_1: Sorbitol	6526.098	1	6526.098	50.714	<0.0001
x_2: Glycerol	3447.240	1	3447.240	26.788	0.0001
$x_1.x_2$	3612.500	1	3612.500	28.073	<0.0001
x_1^2	–	–	–	–	-
x_2^2	788.928	1	788.928	6.130	0.025
Lack of fit	1930.232	4	482.558		
Pure error	0.0000	11	0.0000		
Total error	1930.232	15			
FTT					
x_1: Sorbitol	10,280.109	1	10,280.109	103.854	<0.0001
x_2: Glycerol	2885.108	1	2885.108	29.146	<0.0001
$x_1.x_2$	3612.500	1	3612.500	36.495	<0.0001
x_1^2	–	–	–	–	–
x_2^2	2117.500	1	2117.500	21.392	0.0003
Lack of fit	1484.782	4	371.196		
Pure error	0.0000	11	0.0000		
Total error	1484.782	15			

fact, only the first order terms (x_1 and x_2), GYL binomial term (x_2^2), and their interaction ($x_1.x_2$) demonstrated a significant effect on SIT and FTT with a very low p-value for both MAL and SSOS. In contrast, due to the insignificant impact (p-value >0.1) of SOR quadratic term (x_1^2) on the responses for both types of starch, this term was eliminated from the model.

The regression coefficients and the fit models for SIT (y_1) and FTT (y_2) based on %SOR and %GLY in the SSOS and MAL quadratic model are shown in Eequation 5 (a and b) for SSOS, and Equation. 6 (a and b) for MAL as follows:

$$y_1 = 161.78 - 5.625\,x_1 - 13.428\,x_2 + 13.75\,x_1x_2 - 11.607\,x_2^2 \quad \text{(5-a)}$$

$$y_2 = 183.392 - 12.026\,x_1 - 11.446\,x_2 + 6.25\,x_1x_2 - 10.178\,x_2^2 \quad \text{(5-b)}$$

$$y_1 = 146.785 - 20.196\,x_1 - 14.678\,x_2 + 21.25\,x_1x_2 + 8.392\,x_2^2 \quad \text{(6-a)}$$

$$y_2 = 165 - 25.347\,x_1 - 13.428\,x_2 + 21.25\,x_1x_2 + 13.75\,x_2^2 \quad \text{(6-b)}$$

Based one the model, for SSOS, Equation (5), both SIT and FTT (y_1 and y_2, respectively) indicate that increasing either SOR (x_1) or GYL (x_2) could decrease the respective outcomes, with GYL exerting a more substantial negative influence in SIT value (Equation 5-a). The positive interaction term (x_1x_2) in both equations suggests that when both variables are elevated, they can somewhat offset their individual negative impacts, although the diminishing returns from GYL with the negative coefficient of its quadratic term (x_2^2) highlight the stronger impact of higher GYL concentrations on SIT and FTT reduction for this starch.

For MAL, Equation 6 (a and b), the coefficients show an even stronger negative influence of SOR concentration on SIT and FTT values, while the interaction term remains significant, highlighting the importance of optimizing both variables together to minimize the response. Nevertheless, despite SSOS, the positive quadratic term for GYL (x_2^2) suggests that keeping its amount low may be required to achieve the lowest possible SIT and FTT levels, yet careful management of both variables is essential to meet the objective of achieving the lowest SIT and FTT outputs.

For SSOS results, the findings indicate a robust design performance for predicting the relevant responses, demonstrated by a relatively high correlation coefficient $R^2 = 0.89$ and 0.86 for SIT and FTT, respectively, as shown in Fig. 1(a and b). The closer the R^2 value to 1.00, the higher the quality of the model (Zhang et al., 2024). This figure (Fig. 1a and b) indicates the correlation between the predicted values from Equation (5-a and 5-b) and experimental ones for SSOS starch. The data points show variations close to the diagonal line, suggesting that the model effectively predicts the experimental outcomes and can assist in parameter optimization (Zhang et al., 2024).

To illustrate the interactions between the two independent variables and each response variable, response surface methodologies were developed for each fitted model.

The interaction effects of SOR and GLY on the SIT and FTT are depicted in Fig. 2a and 2b, respectively, using the response surface analysis. In SSOS, the minimum SIT (100 °C) is obtained when SOR and GYL are 0 % and 20 %, respectively, while the lowest FTT (147 °C) is acquired in 20 % of both SOR and GYL.

However, the model exhibits a relatively high level of FTT (151 °C) and SIT (139 °C) for the former and latter, respectively, highlighting them as unfavorable situations. To aim better saleability, both SIT and FTT are crucial to be at their lowest possible level, leading to importance of considering them in the simultaneously.

As shown in the response surface in Fig. 2, by evaluating the impact of SOR and GYL levels on SIT (Fig. 2a) and FTT (Fig. 2b), two analogous types of parabolas are achieved. These parabolic surfaces indicate that by increasing the level of each additive (SOR and GYL) while the other level was maintained, the outcome parameters (SIT and FTT) varied; thereby, in most cases they increased initially and then dropped by adding further amount of the agent. Nonetheless, the reduction part of this pattern was not followed equally by the whole surface and for some additive levels, where SIT or FTT decreased faster comparing to the other ones. Moreover, in case of changing one factor while the other one was also changing, the parabolas indicated different scenarios for each response and every condition. In SSOS, although the impact of GYL (p-value <0.0001) was slightly more significant than SOR (p-value <0.0080) for SIT, these factors indicate similar effects for FTT. Hence, it was essential to find a situation in which both SIT and FTT were at their lowest possible levels.

For MAL, similarly, the results indicate a strong predictive capability of the design, with high correlation coefficients of $R^2 = 0.88$ for SIT and $R^2 = 0.93$ for FTT (Fig. 3(a and b)). Fig. 3 shows this high level of prediction accuracy.

More specifically, Fig. 3 (a) and (b) illustrate the strong correlation between the predicted values from Equations (6-a and 6-b) and the experimental data. The points in the figures hover around the diagonal line, supporting the fact that the model effectively predicts experimental outcomes and is reliable for parameter optimization. Moreover, the effect of SOR and GLY on SIT and FTT in MAL as coating solution is demonstrated in Fig. 4 (a) and 4 (b), respectively.

The response surface depicted in Fig. 4 illustrates the effects of varying levels of SOR and GYL on SIT (Fig. 4a) and FTT (Fig. 4b), resulting in two similar parabolic shapes. Although the parabolas were reasonably alike, they followed different pattern comparing to the observations in SSOS section.

When MAL was utilized, the increase in amount of one plasticizer led to consistent decline in both SIT and FTT levels while the amount of another agent was hold around zero. However, for high concentrations (around 20 %) this trend was reversed in which by increasing the amount of another additive, except for a slight reduction in the outcomes by adding GYL up to 5 % when SOR was maintained at 20 %, both SIT and FTT values were escalated.

Furthermore, when one agent amount was adjusted alongside the other, the surfaces revealed distinct outcomes for each response under varying conditions. The quadratic term of SOR amount played a slightly less significant role comparing to other terms especially in case of SIT level (P-value = 0.025). Therefore, also in MAL family, identification of a condition where both SIT and FTT reached their minimum levels was vital.

The adjusted R-squared (R^2 Adj) values were 0.85 for SIT of SSOS and MAL, and 0.81 and 0.92 for FTT of SSOS and MAL, respectively. This implies that approximately 85 %, 81 %, and 92 % of the variability in the dependent variable can be explained by the independent variables included in the CCD. Indeed, the high R^2 Adj values indicate a strong explanatory power of the regression models, suggesting that the independent variables included in the CCD analysis are effective in predicting the dependent variables (STI and FTT).

In our study, the coefficient of variation (CV%) were 4.825 % and

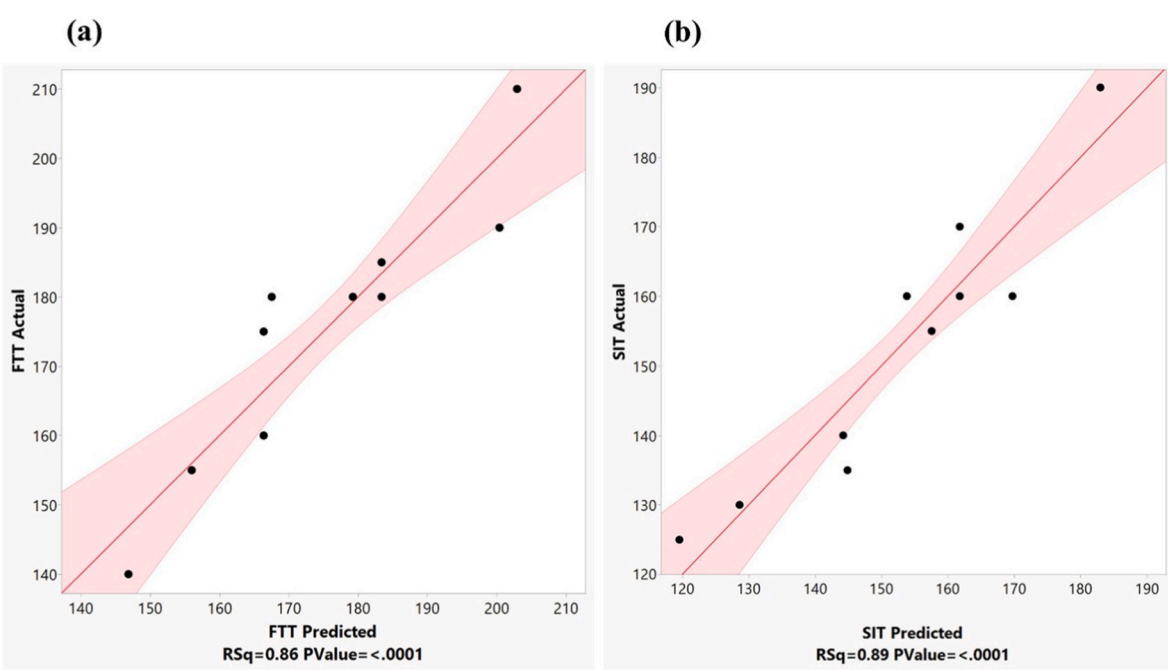

Fig. 1. Analysis of SIT and FTT for SSOS family, (a) actual SIT response versus SIT predict, (b) actual FTT response versus FTT predict.

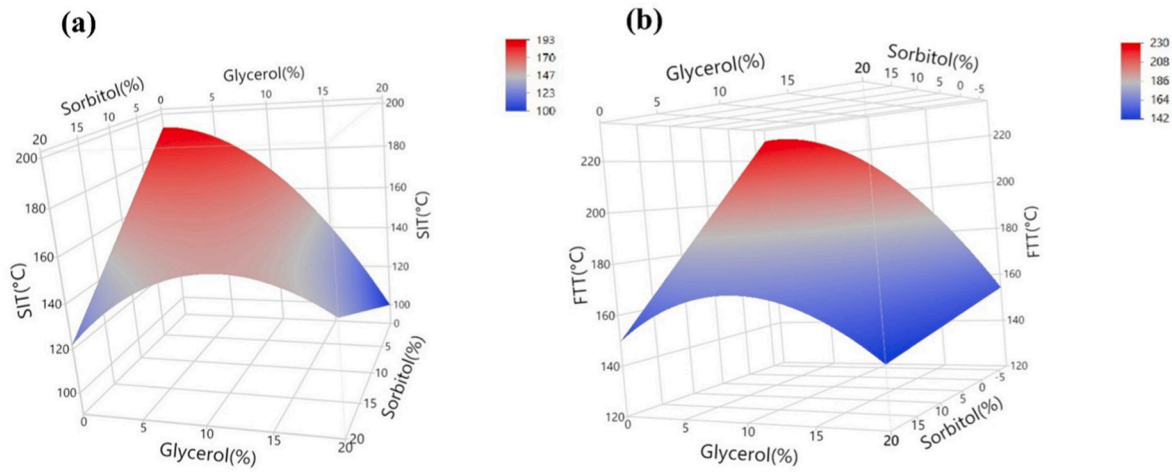

Fig. 2. Analysis of SIT and FTT for SSOS family, (a) response surface for SIT, (b) response surface for FTT.

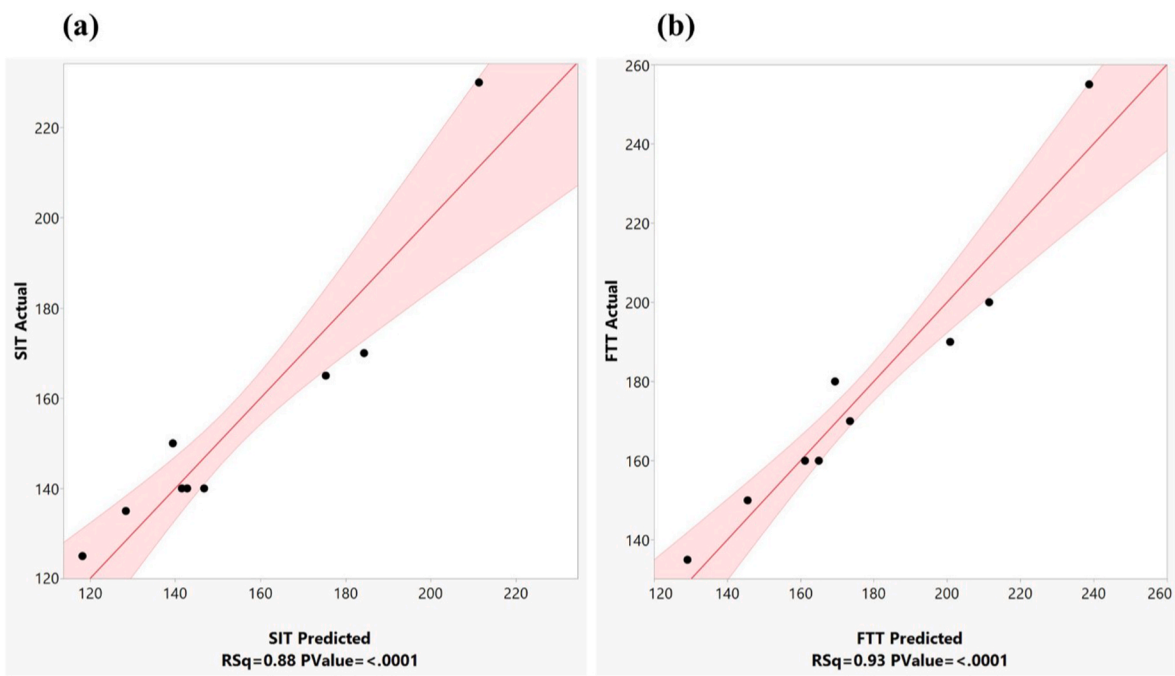

Fig. 3. Analysis of SIT and FTT for MAL family, (a) actual SIT response versus SIT predict, (b) actual FTT response versus FTT predict.

4.636 % for SIT and FTT of SSOS, respectively. Additionally, for MAL, CV% were 7.390 % and 5.652 % for SIT and FTT, respectively. Generally, a CV value below 10 % is preferred, as it indicates high precision and low variability within the dataset (Moussa et al., 2022). Consequently, these results demonstrate the high precision and reproducibility of CCD in optimizing and analyzing the effects of our formulation.

3.1.2. Optimization of coating formulation and experimental validation

The optimization of the coating formulation on paper packaging using CCD aimed to simultaneously minimize the SIT (%) and FTT (%) as much as possible using the desirability score, as shown in Figs. 5 and 6 for SSOS and MAL, respectively. The highest desirability of model was determined to be 99.1 % for the SSOS family and 98.0 % for that of MAL (see Figs. 5 and 6).

In general, the Y-axis displays the response (or desirability), while the X-axis shows the factors. The blue numbers indicate the response ranges achievable with the optimal settings for each factor, and the red number represents. Furthermore, the regions shaded in gray between the blue lines indicate the confidence interval for each graph. The plots at the bottom illustrate the change of desirability score with different level of each factor (Malcı et al., 2022).

The objective was to minimize both SIT and FTT reflected through the maximum desirability scores. For SSOS, the fitting model suggested a coating formulation of 10 % SOR and 20 % GLY with predicted SIT of 120 °C and FTT of 147 °C which interestingly the percentages of GLY and SOR were the same as in run 2 (or 13). In addition, the most desire predicted results for MAL showed 20 % SOR and 5 % GLY with SIT of 112 °C and FTT of 125 °C. In order to verify the model's predictions, the samples were retested using the optimized levels of SOR and GYL for each modified starch family.

The ranges indicated under SIT and FTT for the optimal point represent the 95 % PIs for each response in MAL and SSOS in Figs. 5 and 6, respectively. For SSOS with 10 % SOR and 20 % GYL, SIT was predicted to be in range of 110.9–128.2 °C, while FTT was anticipated to be between 137.3 and 156.4 °C. For the other modified starch, MAL, with 20 % SOR and 5 % GYL as the optimum point, the intervals for SIT and

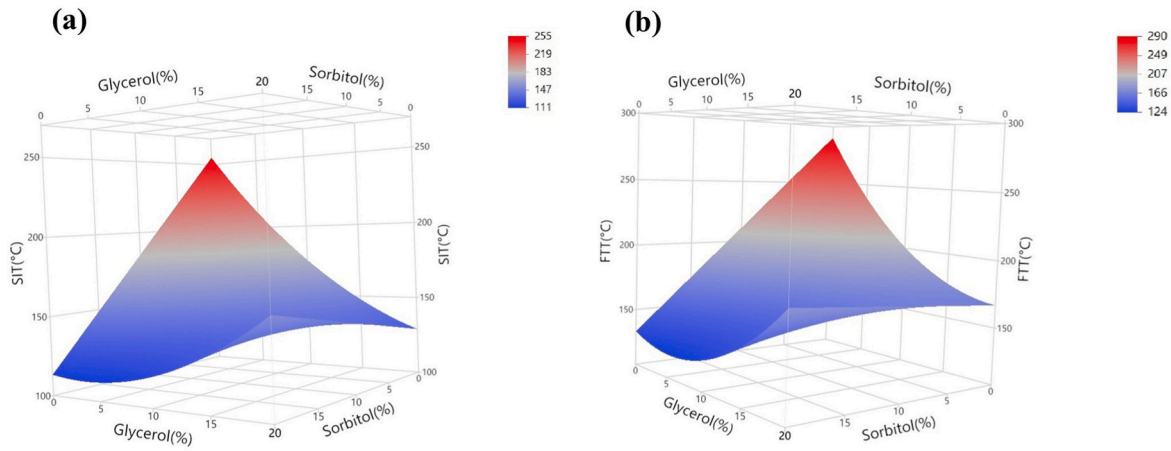

Fig. 4. Analysis of SIT and FTT for MAL family, (a) response surface for SIT, (b) response surface for FTT.

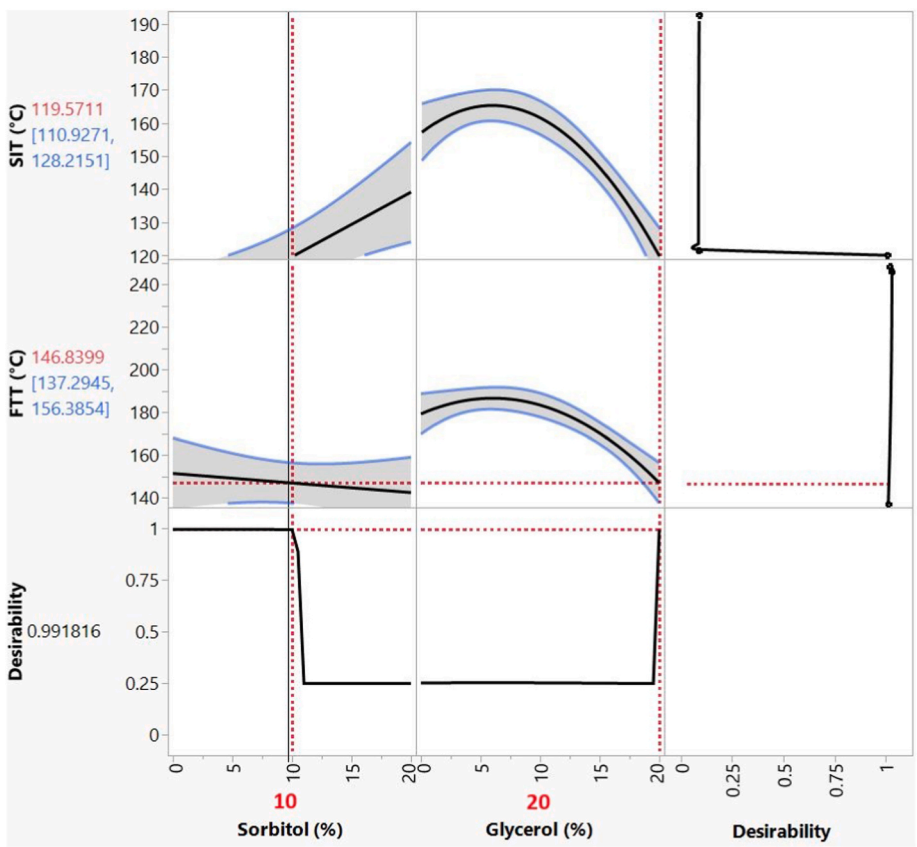

Fig. 5. Profiler and desirability graph for the combined optimization of SIT and FTT in the SSOS.

FTT were obtained to be between 97.5 to 125.4 °C and 111.9–136.6 °C, respectively. Initially, a single confirmation run for each of the two optimum points was performed to measure their FTT and SIT. The results are summarized in Table 4.

As shown in Table 4, all the SIT and FTT results achieved from the one-time confirmation, fell within the PI suggested by the regression. Thus, the model demonstrated high consistency with the experimental values closely matching the predicted ones.

In the second step, as summarized in Table 5, the modified starches, with optimized level of SOR and GYL, were prepared and evaluated with 4 more replications (5 in total) to measure their SIT and FTT and obtain the mean and standard deviation of the confirmation runs.

No block effect was detected, as there was no significant shift in the outcomes of the confirmation runs. All SIT and FTT values remained well within their respective PI ranges, indicating a stable model performance across different conditions. In addition, the confidence intervals calculated using a 99 % confidence limit, further validated the accuracy of the model. Notably, all predicted values fell within the interval surrounding the mean of the confirmation runs. This alignment reinforces the reliability of the model, demonstrating high consistency between the experimental values and the predicted outcomes. Overall, the results illustrate a strong correlation, confirming that the model accurately reflects the underlying processes being studied.

The optimal samples for SSOS and MAL with other favorable samples with relatively acceptable SIT and FTT, and some unfavorable ones with very high SIT and FTT, will be characterized, compared and assessed

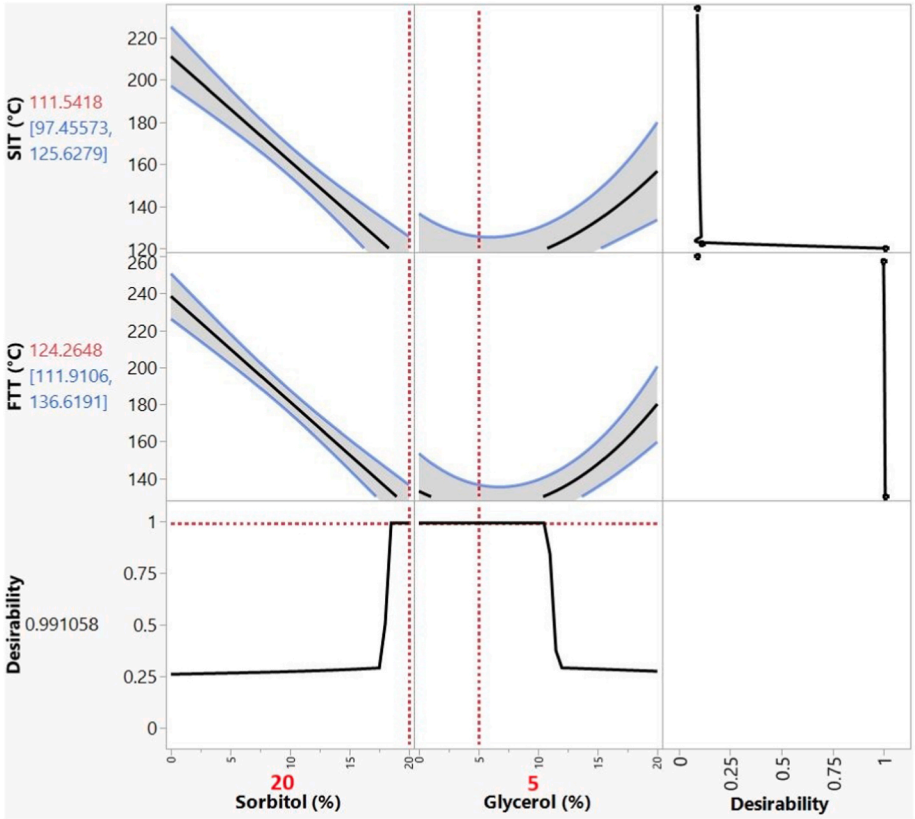

Fig. 6. Profiler and desirability graph for the combined optimization of SIT and FTT in the MAL.

Table 4
Validation of the optimum data using 95 % PI and single confirmation run.

Modified starch	Variable			Predicted values (°C)	Predicted interval (PI) (°C)	Single confirmation run (°C)
	SOR %	GYL %				
SSOS	10	20	SIT	119.6	110.9–128.2	120
			FTT	146.8	137.3–156.4	145
MAL	20	5	SIT	111.6	97.5–125.6	115
			FTT	124.3	111.9–136.6	120

Table 5
Empirical verification of the predicted optimal parameters.

Modified starch	Variable			Predicted values (°C)	Mean of confirmation runs (°C), N = 5	Standard deviation of confirmation runs (°C)	Confidence interval (99 % confidence)
	SOR %	GYL %					
SSOS	10	20	SIT	119.6	121.0	4.2	± 5.6
			FTT	146.8	145.0	5.0	± 6.7
MAL	20	5	SIT	111.6	114.0	4.2	± 5.6
			FTT	124.3	123.0	4.5	± 6.0

more in a future study.

4. Conclusion

The potential of using modified starches, specifically SSOS and MAL, as home compostable coatings to enhance the heat sealability of paper-based food packaging was thoroughly evaluated. Through a designed experimental framework using CCD and RSM, the use of plasticizers, SOR and GLY, was assessed to improve sealing properties. The optimal formulation for SSOS involved 10 % SOR and 20 % GLY, achieving a SIT of 120 °C and an FTT of 147 °C. For MAL, the ideal formulation was 20 % SOR and 5 % GLY, with SIT and FTT values of 112 °C and 125 °C, respectively. These conditions were validated through PI following by single confirmation runs and CI around mean of multiple confirmation runs, verifying that the experimental outcomes fell within the predicted intervals, thereby demonstrating the model's reliability and accuracy.

Statistical analyses revealed significant effects of the plasticizers on SIT and FTT, with high correlation coefficients ($R^2 = 0.89$ for SIT and 0.86 for FTT in SSOS, and $R^2 = 0.88$ for SIT and 0.93 for FTT in MAL), indicating robust predictive capabilities. The adjusted R-squared values further supported the models' explanatory power, with 85 % and 81 % of the variability in SIT and FTT for SSOS, and 92 % for FTT in MAL, were accounted for by the independent variables. The low coefficients of variation (CV%), with values of 4.825 % and 4.636 % for SIT and FTT in

SSOS, and 7.390 % and 5.652 % for SIT and FTT in MAL, obtained in this study indicated the high precision and reproducibility of the experimental design.

These findings highlighted the potential of the modified starch coatings to serve as sustainable alternatives to traditional plastic packaging. The interactions between plasticizer concentrations and sealing performance provided a valuable foundation for future research and commercial applications, promoting the development of packaging solutions that are both environmentally friendly and functionally robust. Overall, this research contributed significantly to advancing sustainable packaging technologies in the food industry, aligned with global sustainability purposes.

CRediT authorship contribution statement

Azadeh Sadeghi: Writing – review & editing, Writing – original draft, Visualization, Validation, Methodology, Investigation, Formal analysis, Data curation, Conceptualization. **Farshad Abavisani:** Writing – original draft, Validation, Methodology, Investigation, Data curation. **Amir Saffar:** Supervision, Project administration, Methodology, Funding acquisition, Conceptualization. **Abdellah Ajji:** Supervision, Project administration, Methodology, Funding acquisition.

Declaration of competing interest

The authors declare the following financial interests/personal relationships which may be considered as potential competing interests: Azadeh Sadeghi reports financial support was provided by Natural Sciences and Engineering Research Council of Canada. Azadeh Sadeghi reports financial support was provided by 3Spack Industrial Research Chair. Azadeh Sadeghi reports financial support was provided by Research Center for High Performance Polymer and Composite Systems (CREPEC). If there are other authors, they declare that they have no known competing financial interests or personal relationships that could have appeared to influence the work reported in this paper.

Acknowledgment

This research was supported by funding from the Natural Sciences and Engineering Research Council of Canada (NSERC), the 3Spack Industrial Research Chair, the Research Center for High Performance Polymer and Composite Systems (CREPEC), the Chemical Engineering Department at Polytechnique Montréal, as well as ProAmpac Flexible Packaging and Prima.

Data availability

No data was used for the research described in the article.

References

Allen, K., 1987. A review of contemporary views of theories of adhesion. J. Adhes. 21 (3–4), 261–277.
Alves, V.D., et al., 2007. Effect of glycerol and amylose enrichment on cassava starch film properties. J. Food Eng. 78 (3), 941–946.
Antony, J., 2023. Design of Experiments for Engineers and Scientists. Elsevier, Amsterdam, Netherlands.
Apriyanto, A., Compart, J., Fettke, J., 2022. A review of starch, a unique biopolymer–Structure, metabolism and in planta modifications. Plant Sci. 318, 111223.
Bagheri, A.R., et al., 2016. Modeling and optimization of simultaneous removal of ternary dyes onto copper sulfide nanoparticles loaded on activated carbon using second-derivative spectrophotometry. J. Taiwan Inst. Chem. Eng. 65, 212–224.
Bamps, B., Buntinx, M., Peeters, R., 2023. Seal materials in flexible plastic food packaging: a review. Packag. Technol. Sci. 36 (7), 507–532.
Basiak, E., Lenart, A., Debeaufort, F., 2018. How glycerol and water contents affect the structural and functional properties of starch-based edible films. Polymers 10 (4), 412.
Coggins, T.L., 2000. Print No more: US code, code of federal regulations, and the federal register. Va. Lawyer 49 (3), 53.
Das, M., Chowdhury, T., 2016. Heat sealing property of starch based self-supporting edible films. Food Packag. Shelf Life 9, 64–68.
Deshwal, G.K., Panjagari, N.R., Alam, T., 2019. An overview of paper and paper based food packaging materials: health safety and environmental concerns. J. Food Sci. Technol. 56, 4391–4403.
Du, Q., et al., 2021. Whey protein and maltodextrin-stabilized oil-in-water emulsions: effects of dextrose equivalent. Food Chem. 339, 128094.
Dudbridge, M., 2016. Handbook of Seal Integrity in the Food Industry.
Frihart, C.R., 2005. Adhesive Bonding and Performance Testing of Bonded Wood Products.
Ganjizadeh Zavareh, S., Javanmard Dakheli, M., Tajeddin, B., 2021. Optimization of biodegradable paper cup packaging coated with whey protein isolate and rice bran wax as potential popcorn package. Food Sci. Nutr. 9 (12), 6762–6775.
Garnero, C., Aloisio, C., Longhi, M.R., 2013. Ibuprofen-maltodextrin Interaction: Study of Enantiomeric Recognition and Complex Characterization.
Hauptmann, M., et al., 2021. The effect of flexible sealing jaws on the tightness of pouches made from mono-polyolefin films and functional papers. Packag. Technol. Sci. 34 (3), 175–186.
He, R., et al., 2023. Starch modification with molecular transformation, physicochemical characteristics, and industrial usability: a state-of-the-art review. Polymers 15 (13), 2935.
Herrera, N., et al., 2016. Functionalized blown films of plasticized polylactic acid/chitin nanocomposite: preparation and characterization. Mater. Des. 92, 846–852.
Ilhan, I., et al., 2021. Understanding the factors affecting the seal integrity in heat sealed flexible food packages: a review. Packag. Technol. Sci. 34 (6), 321–337.
Jadaa, W., Prakash, A., Ray, A.K., 2020. Modeling of degradation of Diazo dye in swirl-flow photocatalytic reactor: response surface approach. Catalysts 10 (12), 1418.
Jahdkaran, E., et al., 2021. The effects of methylcellulose coating containing carvacrol or menthol on the physicochemical, mechanical, and antimicrobial activity of polyethylene films. Food Sci. Nutr. 9 (5), 2768–2778.
Jiménez, A., et al., 2013. Phase transitions in starch based films containing fatty acids. Effect on water sorption and mechanical behaviour. Food Hydrocoll. 30 (1), 408–418.
Kavčič, U., Lavrič, G., Karlovits, I., 2023. Alternative fiber-based paperboard adhesion evaluation with T-and Y-peel testing. Appl. Sci. 13 (17), 9779.
Lim, W.S., et al., 2020. Heat-sealing property of cassava starch film plasticized with glycerol and sorbitol. Food Packag. Shelf Life 26, 100556.
Liu, Z., et al., 2013. Edible starch sodium octenyl succinate film formation and its physical properties. J. Appl. Polym. Sci. 127 (4), 2922–2927.
Malcı, K., Walls, L.E., Rios-Solis, L., 2022. Rational design of CRISPR/Cas12a-RPA based one-pot COVID-19 detection with design of experiments. ACS Synth. Biol. 11 (4), 1555–1567.
Mee, R.W., 2009. A Comprehensive Guide to Factorial Two-Level Experimentation. Springer.
Merabtene, M., et al., 2022. Heat sealing evaluation and runnability issues of flexible paper materials in a vertical form fill seal packaging machine. Bioresources 17 (1), 223.
Mohammadi Nafchi Abdorreza, M.N.A., Cheng, L., Karim, A., 2010. Effects of Plasticizers on Thermal Properties and Heat Sealability of Sago Starch Films.
Montgomery, D.C., 2017. Design and Analysis of Experiments. John Wiley & Sons, Inc., Hoboken, NJ.
Morris, B., 2017. Thermoforming, orientation, and shrink. The Science and Technology of Flexible Packaging: Multilayer Films from Resin and Process to End Use Plastics Design Library, pp. 401–433.
Morris, B.A., 2022. The Science and Technology of Flexible Packaging: Multilayer Films from Resin and Process to End Use. William Andrew.
Moussa, H., et al., 2022. Definitive screening design and I-optimal design for optimization of ultrasound-assisted extraction of phenolic content and antioxidant capacity from Salvia officinalis L. leaves. Sustain. Chem. Pharm. 29, 100820.
Muscat, D., et al., 2012. Comparative study of film forming behaviour of low and high amylose starches using glycerol and xylitol as plasticizers. J. Food Eng. 109 (2), 189–201.
Myers, R.H., 2016. Response Surface Methodology Process and Product Optimization Using Designed Experiments. John Wiley & Sons, Hoboken, New Jersey, USA. Incorporated: John Wiley & Sons, Inc.
Nechita, P., Roman, M., 2020. Review on polysaccharides Used in Coatings for food packaging papers. Coatings 10 (6), 566.
Parikh, A., Agarwal, S., Raut, K., 2014. A review on applications of maltodextrin in pharmaceutical industry. System 4 (6).
Piergiovanni, L., Limbo, S., 2016. Food Packaging Materials. Springer.
Rompothi, O., et al., 2017. Development of non-water soluble, ductile mung bean starch based edible film with oxygen barrier and heat sealability. Carbohydr. Polym. 157, 748–756.
Saavedra-Leos, Z., et al., 2015. Technological application of maltodextrins according to the degree of polymerization. Molecules 20 (12), 21067–21081.
Sajilata, M., Singhal, R.S., 2005. Specialty starches for snack foods. Carbohydr. Polym. 59 (2), 131–151.
Salwa, H., et al., 2019. Green bio composites for food packaging. Int. J. Recent Technol. Eng. 8 (2), 450–459.
Sudarjanto, G., Keller-Lehmann, B., Keller, J., 2006. Optimization of integrated chemical–biological degradation of a reactive azo dye using response surface methodology. J. Hazard Mater. 138 (1), 160–168.
Suh, J.H., et al., 2020. Effect of moisture content on the heat-sealing property of starch films from different botanical sources. Polym. Test. 89, 106612.
Thurber, H., Curtzwiler, G.W., 2020. Suitability of poly (butylene succinate) as a coating for paperboard convenience food packaging. Int. J. Biobased Plastics. 2 (1), 1–12.

Wang, X., et al., 2011. Preparation and characterisation of octenyl succinate starch as a delivery carrier for bioactive food components. Food Chem. 126 (3), 1218–1225.
Xiao, Z., et al., 2022. Maltodextrin as wall material for microcapsules: a review. Carbohydr. Polym. 298, 120113.
Zamani, Z., Razavi, S.M.A., 2023. Steady shear rheological properties, microstructure and stability of water in water emulsions made with basil seed gum and waxy corn starch or high pressure-treated waxy corn starch. LWT 174, 114453.
Zhang, S., et al., 2024. Modelling and optimization of electrodeposited amorphous Fe-P alloys using central composite design and response surface method. Int. J. Electrochem. Sci. 19 (7), 100644.